Published in Chemistry of Materials 17, issue 19, pp. 4798–4807, 2005,
which should be used for any reference to this work

Mesomorphic Hexabenzocoronenes Bearing Perfluorinated Chains

Bassam Alameddine,[†] Olivier F. Aebischer,[†] Walter Amrein,[‡] Bertrand Donnio,[§] Robert Deschenaux,[||] Daniel Guillon,[§] Corinne Savary,[†] David Scanu,[||] Oliver Scheidegger,[‡] and Titus A. Jenny*,[†]

Chemistry Department, University of Fribourg, 9 chemin du Musée, CH-1700 Fribourg, Switzerland, Laboratory of Organic Chemistry, Wolfgang-Pauli-Str. 10, ETH Hönggerberg, CH-8093 Zurich, Switzerland, Institut de Physique et Chimie des Matériaux de Strasbourg - IPCMS, Groupe des Matériaux Organiques - GMO, UMR 7504 - CNRS/Université Louis Pasteur, 23, rue du Loess, BP 43, F-67034 Strasbourg Cedex 2, France, and Institute of Chemistry, University of Neuchâtel, 51 Av. du Bellevaux, CH-2007 Neuchâtel, Switzerland

Synthesis and characterization of new hexabenzocoronene (HBC) derivatives bearing perfluoroalkylated chains are described. These disc-shaped polycondensed aromatic hydrocarbons are known to self-assemble by π-stacking into columnar architectures. The peripheral decoration with perfluorinated chains, well-known for their low van der Waals forces, leads as expected to reduced intercolumnar interactions. Powder X-ray diffraction and differential scanning calorimetry of these perfluoroalkylated HBCs proved liquid crystalline (LC) properties whose transition temperatures, mesophase stability, and nature depend on the detailed structure of these side chains, i.e., the ratio between aliphatic and perfluorinated parts. On the other hand, the insertion of a phenyl spacer between the aromatic core and the lateral chains increases the LC transition temperature and, surprisingly, switches the mesophase structure from columnar to smectic.

Introduction

Extended polyaromatic hydrocarbons (PAH) are finding increasing interest among other self-assembled supramolecular systems due to their pronounced tendency for formation of extended π-stacked assemblies. These have many potential properties, such as a high electron density which allows their use in promising applications in molecular electronics.[1] However, the main drawback of these rigid polycondensed molecules resides in the difficulty of their synthesis and their very low solubility which prevents their isolation and manipulation. Recently, Müllen and co-workers[2] succeeded in finding a versatile synthesis of hexa-*peri*-hexabenzocoronene (HBC), a polycondensed hexagonal molecule containing 13 benzene rings which shows a very high chemical stability[3] and which self-organizes into columnar stacks, by π-stacking, with an outstanding degree of order in the solid state.[4,5] Additionally, its solubility was improved by the addition of peripheral long aliphatic chains which at the same time bestows the molecule with a ditopic property: These HBC derivatives show a liquid crystalline (LC) state over a wide temperature range depending on the length of the aliphatic chain.[6] Moreover, these HBC derivatives exhibit the highest charge carrier mobility recorded so far for an organic molecule both in the solid and in the liquid crystalline states,[7] paving the way toward their application in the domain of electronic[8] and optoelectronic[9−11] devices.

Nevertheless, the lateral interaction between the adjacent HBC stacks caused by the crystalline packing of their aliphatic side chains[12] constitutes a major drawback since it interferes with the formation of very long conducting π-stacks. Additionally, most of the HBCs bearing aliphatic chains are liquid crystalline just above room temperature, which leads to a second disadvantage since it induces a drastic decrease of their charge carrier mobilities,[13] which is reported to be due to "lateral" conduction and as a reason for the perturbation or the deterioration of an ideal liquid crystalline mesophase that dominates the conduction process.[14]

* To whom correspondence should be addressed. Tel. (Office): +41(0)-263008778. Fax: +41(0)263009739. E-mail: titus.jenny@unifr.ch.
[†] University of Fribourg.
[‡] ETH Hönggerberg.
[§] CNRS/Université Louis Pasteur.
[||] University of Neuchâtel.

(1) Bushby, R. J.; Lozman, O. R. *Curr. Opin. Colloid Interface Sci.* **2002**, *7*, 343−354.
(2) Keegstra, M. A.; de Feyter, F.; de Schryver, F. C.; Müllen, K. *Angew. Chem., Int. Ed. Engl.* **1996**, *35*, 774−776.
(3) Clar, E.; Ironside, C. T.; Zander, M. *J. Chem. Soc.* **1959**, *1*, 142−147.
(4) Ruffieux, P.; Gröening, O.; Bielman, M.; Simpson, C.; Müllen, K.; Schlapbach, L.; Gröening, P. *Phys. Rev. B* **2002**, *66*, 073409/073401−073409/073404.
(5) Bunk, O.; Nielsen, M. M.; Solling, T. I.; Van de Craats, A.; Stutzmann, N. *J. Am. Chem. Soc.* **2003**, *125*, 2252−2258.
(6) Herwig, P.; Kayser, C. W.; Müllen, K.; Spiess, H. W. *Adv. Mater.* **1996**, *8*, 510−513.
(7) Van de Craats, A.; Warman, J. M. *Adv. Mater.* **2001**, *13*, 130−133.
(8) Van de Craats, A.; Stutzman, N.; Bunk, O.; Nielsen, M. M.; Watson, M.; Müllen, K.; Chanzy, H. D.; Sirringhaus, H.; Friend, R. H. *Adv. Mater.* **2003**, *15*, 495−499.
(9) Liu, C.-Y.; Fechtenkötter, A.; Watson, M. D.; Müllen, K.; Bard, A. J. *Chem. Mater.* **2003**, *15*, 124−130.
(10) Schmidt-Mende, L.; Fechtenchötter, A.; Müllen, K.; Moons, E.; Friend, R. H.; MacKenzie, J. D. *Science* **2001**, *293*, 1119−1122.
(11) O'Neill, M.; Kelly, S. M. *Adv. Mater.* **2003**, *15*, 1135−1146.
(12) Ito, S.; Wehmeier, M.; Brand, J. D.; Kübel, C.; Epsch, R.; Rabe, J. P.; Müllen, K. *Chem. Eur. J.* **2000**, *6*, 4327−4342.
(13) Van de Craats, A.; Warman, J. M.; Fechtenkötter, A.; Brand, J. D.; Müllen, K. *Adv. Mater.* **1999**, *11*, 1469−1472.
(14) Schouten, P. G.; Warman, J. M.; De Haas, M. P.; Van der Pol, J. F.; Zwikker, J. W. *J. Am. Chem.* Soc. **1992**, *114*, 9028−9034.

Scheme 1. Attempted Synthesis of HBC Bearing Trifluoromethyl or Phenyl Perfluoroalkyl Groups: (a) TMSA, $Pd(PPh_3)_2Cl_2$, CuI, Ph_3P, Piperidine, (b) NaOH, BTACl, CH_2Cl_2, (c) 1 or 2, $Pd(PPh_3)_4$, CuI, Piperidine, (d) $Co_2(CO)_8$, Dioxane, Reflux, (e) $FeCl_3$, CH_3NO_2, CH_2Cl_2, RT, and (f) $AlCl_3$, $Cu(OTf)_2$, CS_2, 30 °C

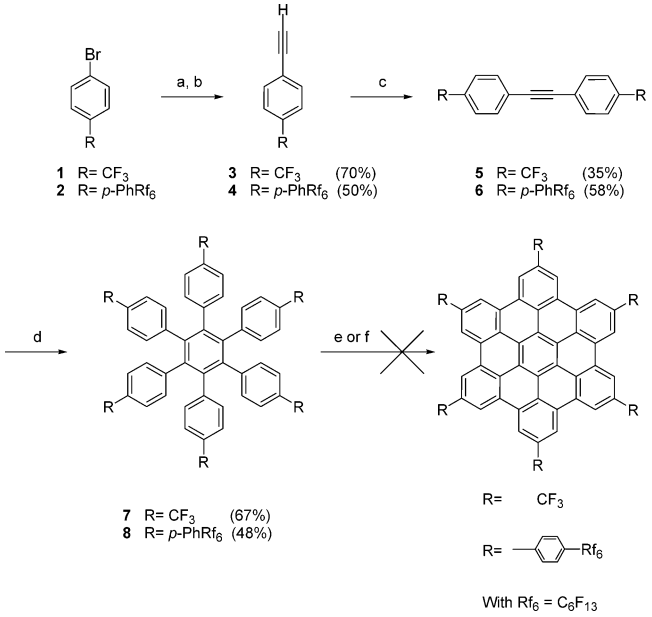

We report herein the synthesis and the characterization of new HBC derivatives that contain long perfluoroalkylated side chains. Based on the preliminary observations of the effect of introducing perfluorinated chains to small discotic systems,[15,16] this seemingly minor change is expected to prevent, or greatly reduce, the intercolumnar interactions by microphase segregation, and hence to increase the one-dimensional charge carrier mobility. The perfluorinated groups are well-known for their Teflon-like properties such as high volatility, high thermal stability, and low aggregation tendency due to their low van der Waals interactions.[17] The introduction of the perfluoroalkylated chains onto the HBC core is, therefore, expected to constitute an isolating "mantle" around the central π-stacked part of the aggregates and to facilitate their self-organization into single dispersed columns.

Synthesis and Characterization

Preparation of HBC with Perfluoroalkylated Chains. It rapidly appeared that the direct attachment of perfluoroalkylated substituents onto the HBC core prevents the formation of the target molecule at the last step of the synthesis (Scheme 1): the high electron-withdrawing effect of trifluoromethyl or perfluoroalkyl groups prevents the cyclodehydrogenation reaction, the key step for obtaining any HBC derivative. Neither of the two known conditions for this reaction, either the mild $FeCl_3/CH_3NO_2$ combination[18] or the harsher $AlCl_3/Cu(OTf)_2$ mixture[19] is effective (Scheme 1). This finding is supported by the recent results of Wu and co-workers,[20] reporting the impossibility to aromatize many hexaphenylbenzene derivatives to their HBC homologues when these former bear strong electron-withdrawing groups. We found that the same result holds even for derivatives in which a phenyl spacer is inserted between the hexaphenylbenzene core and the perfluorinated substituent, revealing, therefore, that the addition of a phenyl intercalator does not reduce the electron-withdrawing effect of the side chain sufficiently. Consequently, we decided to insert an aliphatic spacer between the hexaphenylbenzene core and the perfluoroalkyl chain. In the first attempts, an ethylene spacer was introduced, with or without an additional phenyl spacer, leading successfully to the desired compounds HBC−$Rf_{2,8}$ (**19**) and HBC−$PhRf_{2,8}$ (**20**), respectively (Scheme 2).

The synthesis of HBC−$Rf_{2,8}$ (**19**) and HBC−$PhRf_{2,8}$ (**20**) followed the strategy shown in Scheme 2. 4-Bromo-4′-aminobiphenyl **10** was transformed into the brominated perfluoro-compound **12** in analogy to the diazotization of 4-bromoaniline[21] by preparing its stable tetrafluoroborate diazonium salt first. The diazo derivative was then coupled with 1*H*,1*H*,2*H*-perfluorodecene using ligandless Heck conditions and the resulting perfluorinated trans-olefin derivative was hydrogenated to its aliphatic homologue **12** using a mild Rh/C catalyst, as described for the transformation of **9** into **11**,[22] in 86% overall yield. Both products **11** and **12** were reacted, in a next step, with trimethylsilyl acetylene (TMSA), under suitable Sonogashira cross-coupling reaction conditions.[23,24] Desilylation of the protected acetylene derivatives proved to be difficult and was finally achieved under basic conditions in the presence of a phase transfer catalyst (PTC) to afford products **13** and **14** in moderate yields. Other usual conditions, such as KF or the employment of different mixtures of solvents (MeOH, DMF, and CH_2Cl_2) with or without the presence of a PTC, either proved to be ineffective or led to inseparable mixtures of partially deprotected material. Coupling of **11** with **13**, and **12** with **14**, afforded the tolane species **15** and **16** in 57 and 61%, respectively. Subsequent trimerization, using a catalytic amount of dicobalt carbonyl in refluxing dioxane,[25] yields the perfluorinated hexaaryl benzene derivatives **17** and **18** in 49 and 66%, respectively. The cyclodehydrogenation of **17** was successful only when the more reactive $AlCl_3/Cu(OTf)_2$ combination was used (Table 1, entry 2). Employing the mild $FeCl_3/CH_3NO_2$ combination did not allow the reaction to proceed, even after a long reaction time (entry 1), and only the starting material was recovered. The desired HBC product **19** is obtained after exhaustive washings with aqueous and organic solvents to remove any trace of metallic species and undesired organic compounds. In contrast, the phenyl spaced derivative **18** affords only trace amounts of the desired HBC product (<1%) with the $FeCl_3/CH_3NO_2$ mixture after refluxing the reaction mixture (entry 3). Consequently, application of the harsher Al(III)/Cu(II) conditions produced the desired product **20** in good yield (entry 4). It appears that an ethylene spacer does not fully isolate the electron-withdrawing effect of a perfluoroalkylated chain since the corresponding alkylated products were obtained in very good yields[6] even under the milder $FeCl_3/CH_3NO_2$ conditions.[26]

(15) Dahn, U.; Erdelen, C.; Ringsdorf, H.; Festag, R.; Wendorff, J. H.; Heiney, P. A.; Maliszewskyj, N. C. *Liq. Cryst.* **1995**, *19*, 759−764.
(16) Terasawa, N.; Monobe, H.; Kiyohara, K.; Shimizu, Y. *Chem. Commun.* **2003**, 1678−1679.
(17) Visjager, J.; Tervort, T. A.; Smith, P. *Polymer* **1999**, *40*, 4533−4542.
(18) Kovacic, P.; Jones, M. B. *Chem. Rev.* **1987**, *87*, 357−379 and references therein.
(19) Simpson, C. D.; Brand, J. D.; Berresheim, A. J.; Pryzbilla, L.; Räder, H. J.; Müllen, K. *Chem. Eur. J.* **2002**, *8*, 1424−1429.
(20) Wu, J.; Watson, M. D.; Zhang, L.; Wang, Z.; Müllen, K. *J. Am. Chem. Soc.* **2004**, *126*, 177−186.
(21) Roe, A. *Org. React.* **1949**, *5*, 193−228.
(22) Darses, S.; Pucheault, M.; Genêt, J.-P. *Eur. J. Org. Chem.* **2001**, 1121−1128.
(23) Takahashi, S.; Kuroyama, Y.; Sonogashira, K.; Hagihara, N. *Synthesis* **1980**, 627−629.
(24) Alami, M.; Ferri, F.; Linstrumelle, G. *Tetrahedron Lett.* **1993**, *34*, 6403−6406.
(25) Funk, R. F.; Peter, K.; Volhardt, C. *J. Am. Chem. Soc.* **1980**, *102*, 5253−5261.
(26) Fechtenkötter, A.; Saalwächter, K.; Harbison, M. A.; Müllen, K.; Spiess, H. W. *Angew. Chem., Int. Ed.* **1999**, *38*, 3039−3042.

Scheme 2. Synthesis of HBC−$Rf_{2,8}$ and HBC−$PhRf_{2,8}$: (a) HBF_4, $NaNO_2$, RT, (b) Perfluorodecene, $Pd(OAc)_2$, (c) Rh/C, H_2 (50 atm), CH_2Cl_2, RT, (d) TMSA, $Pd(PPh_3)_2Cl_2$, CuI, Ph_3P, Piperidine, (e) NaOH, BTACl, CH_2Cl_2, MeOH, (f) 11 or 12, $Pd(PPh_3)_4$, CuI, Piperidine, (g) $Co_2(CO)_8$, Dioxane, Reflux, and (h) $AlCl_3$, $Cu(OTf)_2$, CS_2, 30 °C

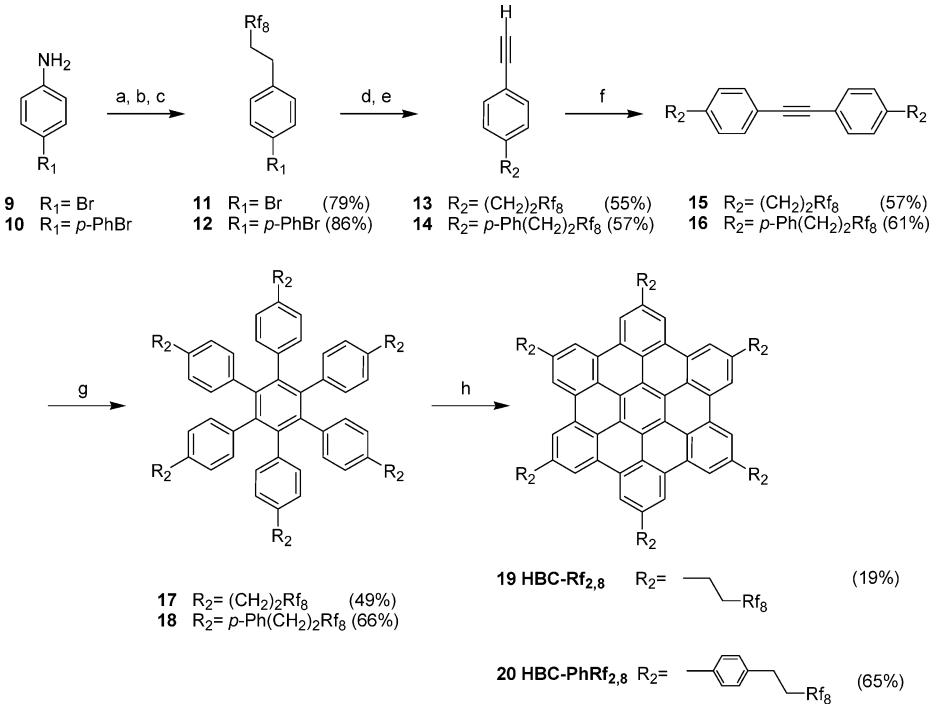

Table 1. Cyclodehydrogenation Reactions of 17 and 18[a]

entry	substrate	reagent (nb. eq/H)	additive	solvent	temp. (°C)	time (h)	product (% yield)
1	**17**	$FeCl_3$(6)	CH_3NO_2	CH_2Cl_2	RT	34[b]	
2	**17**	$AlCl_3$(3.3)[c]	$Cu(OTf)_2$	CS_2	35	24	19 (19)
3	**18**	$FeCl_3$(6)	CH_3NO_2	CH_2Cl_2	RT-reflux	18[d]	20 (<1)
4	**18**	$AlCl_3$(3.3)[c]	$Cu(OTf)_2$	CS_2	35	24	20 (65)

[a] All the reactions were done under argon. [b] Argon was bubbled for 24 h. [c] Equimolar amount of Al/Cu. [d] Argon was bubbled for 17 h followed by reflux for 1 h.

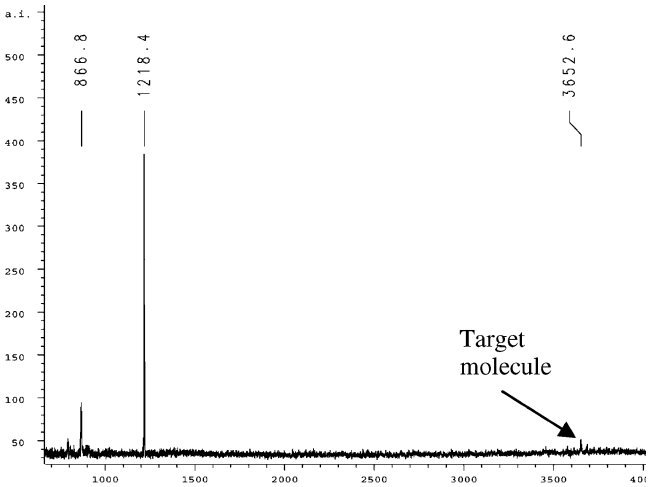

Figure 1. MALDI-TOF spectrum of HBC−$PhRf_{2,8}$ (**20**).

It must be pointed out, however, that both products HBC−$Rf_{2,8}$ and HBC−$PhRf_{2,8}$ display a very low solubility, which leaves MALDI-TOF as the only technique to detect the presence of the desired products (Figure 1) using the same special sample preparation method reported in the literature,[27] but employing the more efficient DCTB matrix.[28]

In an attempt to decouple the perfluoroalkyl chains totally from the HBC core, we synthesized the HBC−$Rf_{4,8}$ (**28**) and HBC−$Rf_{6,6}$ (**29**) derivatives bearing perfluoroalkylated side chains with alkyl intercalators of four and six aliphatic carbons, respectively, in a scheme requiring fewer steps (Scheme 3). The Grignard derivatives **22.1** and **23.1**, prepared from the known bromo perfluoroalkylated chains bearing four and six methylene spacers[29,30] **22** and **23**, were reacted with 4,4′-dibromotolane[31] **21**, under standard Kumada cross-coupling conditions,[32] to afford the corresponding perfluoroalkylated tolane building blocks **24** and **25** in 75 and 65% yield, respectively. Trimerization of the diphenyl acetylene by cobalt catalysis yielded the desired hexaphenyl benzene derivatives **26** and **27** in 70 and 80% yield, respectively. Finally, the aromatization in the presence of the mild $FeCl_3/CH_3NO_2$ reagent produced the corresponding HBCs in 35 and 87% yield, respectively. The $FeCl_3/CH_3NO_2$ mixture was used instead of the $AlCl_3/Cu(OTf)_2$ one in order to prevent any migration or cleavage of the perfluoroalkylated chains as reported in the case of alkylated HBCs.[33]

(27) Pryzbilla, L.; Brand, J.-D.; Yoshimura, K.; Räder, H. J.; Müllen, K. *Anal. Chem.* **2000**, *72*, 4591−4597.
(28) Ulmer, L.; Mattay, J.; Torres-Garcia, H. G.; Luftmann, H. *Eur. J. Mass Spectrom.* **2000**, *6*, 49−52.
(29) Johansson, G.; Percec, V.; Ungar, G.; Zhou, J. P. *Macromolecules* **1996**, *29*, 646−660.
(30) Johansson, G.; Percec, V.; Ungar, G.; Smith, K. *Chem. Mater.* **1997**, *9*, 164−175.
(31) Harisson, R. M.; Brotin, T.; Noll, B. C.; Michel, J. *Organometallics* **1997**, *16*, 3401−3412.
(32) Hayashi, T.; Konishi, M.; Kobori, Y.; Kumada, M.; Higushi, T.; Hirotsu, K. *J. Am. Chem. Soc.* **1984**, *106*, 158−163.

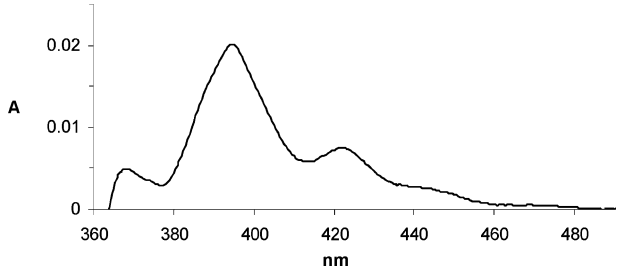

Figure 2. UV−Vis spectrum of HBC−$Rf_{6,6}$ (**29**).

Scheme 3. Synthesis of HBC−$Rf_{4,8}$ (28) and HBC−$Rf_{6,6}$ (29): (a) $Pd(dppf)Cl_2.CH_2Cl_2$, THF, Reflux, (b) $Co_2(CO)_8$, Dioxane, Reflux, and (c) $FeCl_3$, CH_3NO_2, CH_2Cl_2, RT

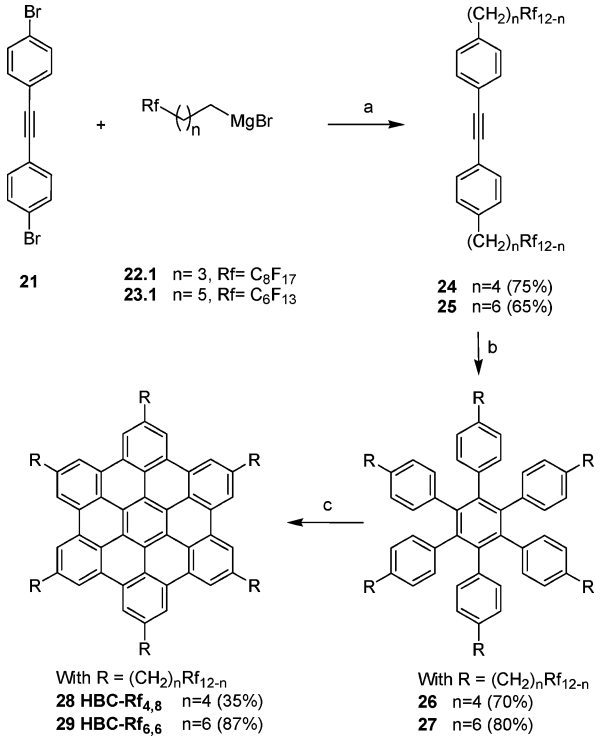

The considerable higher solubility of HBC−$Rf_{4,8}$ (**28**) and HBC−$Rf_{6,6}$ (**29**) as compared to HBC−$Rf_{2,8}$ (**19**) and HBC−$PhRf_{2,8}$ (**20**) allows for UV−Vis spectroscopy of the former. Figure 2 shows the spectrum of a dilute solution of HBC−$Rf_{6,6}$ (**29**) in 1,2,4-trichlorobenzene, which reveals a typical aggregation pattern as has been reported previously.[34]

Preparation of HBC with Perfluoroalkyl-oxy-phenyl Groups. Since the synthesis of HBC derivatives bearing alkoxy side chains was reported to fail due the formation of quinonoid structures,[35] and that of HBC with phenyl oligoether substituents is known,[36] we included the synthesis of HBC molecules bearing perfluorinated alkoxy phenyl groups in our study. Scheme 4 illustrates the two different strategies we employed to produce the required perfluorinated-oxy-diaryl acetylenes: the first pathway consisted of reacting 4-bromo-4′-hydroxy-biphenyl **30** with the perfluorinated

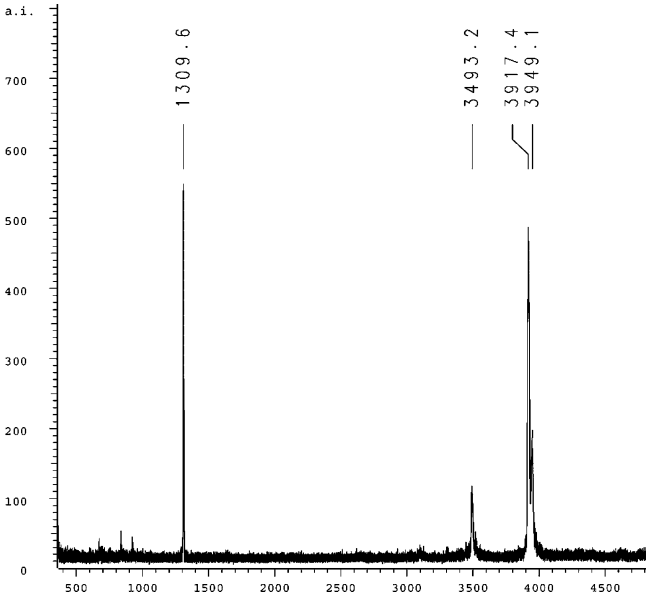

Figure 3. MALDI-TOF of HBC−$PhORf_{4,8}$ (**44**).

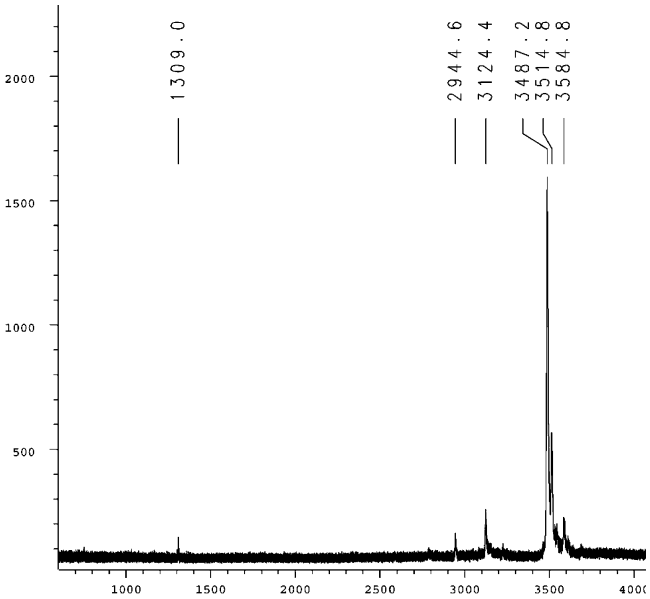

Figure 4. MALDI-TOF of HBC−$PhORf_{6,6}$ (**45**).

chains **22** or **23** in DMF under basic conditions to yield the para-substituted perfluorinated-oxy-bromobiphenyl building blocks **31** and **32** in good yields. Both products were separately transformed, in a step by step Sonogashira cross-coupling reaction scheme under standard palladium conditions, to their corresponding diaryl acetylene homologues **37** and **38** in moderate yields. In a second approach, 4-bromophenol **39** was reacted with **22** under basic conditions to afford the para- substituted perfluoroalkoxy bromobenzene **40** which was converted, in a second step, to its boronic acid derivative **41** in poor yield. The reaction of the latter product with 4,4′-dibromotolane **21**, using Suzuki cross-coupling conditions,[37] was carried out yielding the corresponding tolane product **37** in a fair yield. Even though the second pathway requires less reaction steps than the first one, its overall yield is considerably lower than the latter (23% vs 39%). Products **37** and **38** were trimerized using the standard conditions to afford the desired hexaaryl benzenes **42** and **43**. Cyclodehydrogenation of both products using the mild $FeCl_3/CH_3NO_2$ reagent mixture yields the

(33) Dötz, F.; Brand, J. D.; Ito, S.; Gherghel, L.; Müllen, K. *J. Am. Chem. Soc.* **2000**, *122*, 7707−7717.
(34) Fleming, A. J.; Coleman, J. N.; Dalton, A. B.; Fechtenkötter, A.; Watson, M. D.; Müllen, K.; Byrne, H. J.; Blau, W. J. *J. Phys. Chem. B* **2003**, *107*, 37−43.
(35) Weiss, K.; Beernink, G.; Dötz, F.; Birkner, A.; Müllen, K.; Wöll, C. *Angew. Chem., Int. Ed.* **1999**, *38*, 3748−3752.
(36) Lee, M.; Kim, J.-W.; Peleshanko, S.; Larson, K.; Yoo, Y.-S.; Vaknin, D.; Markutsya, S.; Tsukruk, V. V. *J. Am. Chem. Soc.* **2002**, *124*, 9121−9128.
(37) Miyaura, N.; Yanagai, T.; Suzuki, A. *Synth. Commun.* **1981**, *11*, 513.

Scheme 4. Synthesis of Diaryl Acetylene Bearing Perfluorinated Alkoxy Side Chains: (a) 22 or 23, K_2CO_3, DMF, 80 °C, (b) TMSA, $Pd(PPh_3)_2Cl_2$, CuI, Ph_3P, Piperidine, (c) NaOH, BTACl, CH_2Cl_2, RT, (d) 31 or 32, $Pd(PPh_3)_4$, CuI, Piperidine, (e) 22, K_2CO_3, DMF, 80 °C, 83%, (f) *n*-BuLi, THF, −78 to −40 °C, (g) $B(OMe)_3$, −78 to RT, (h) HCl, 2M, 44%, and (i) 21, $Pd(PPh_3)_4$, Toluene, MeOH, H_2O, K_2CO_3, Reflux

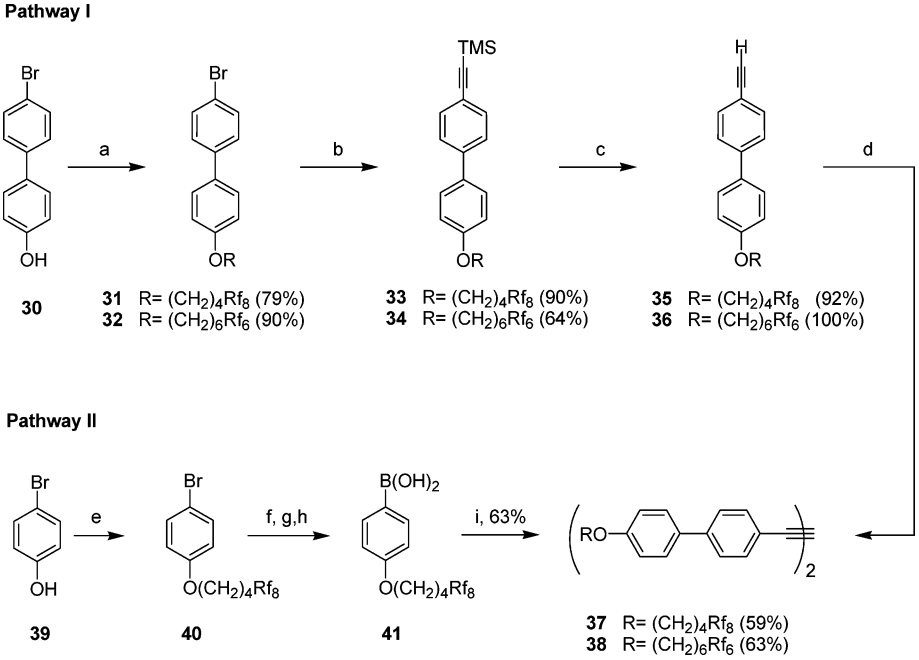

Scheme 5. Synthesis of HBC−$PhORf_{4,8}$ and HBC−$PhORf_{6,6}$: (a) $Co_2(CO)_8$, Dioxane, Reflux and (h) $FeCl_3$, CH_3NO_2, CH_2Cl_2, RT

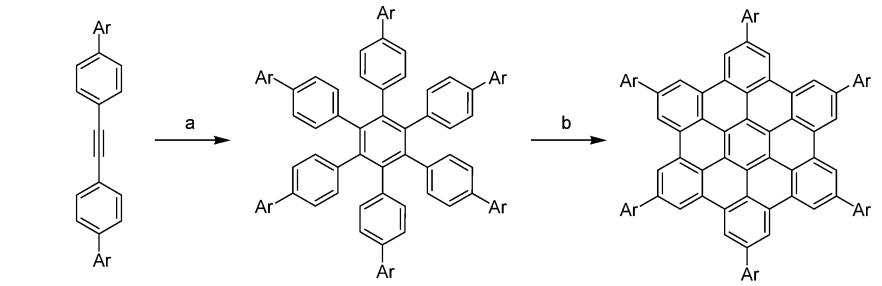

desired HBC derivatives bearing alkoxy side chains HBC−$PhORf_{4,8}$ (**44**) and HBC−$PhORf_{6,6}$ (**45**) in fair to good yield (Scheme 5).

Both HBCs **44** and **45** were characterized by MALDI-TOF mass spectrometry employing the same conditions used for the previous samples (Figures 3 and 4). Again, the HBC−$PhORf_{6,6}$ (**45**) and HBC−$PhORf_{4,8}$ (**44**) differ considerably in their solubility. Whereas the solubility of the former allows for measuring a UV−Vis spectrum in 1,2,4-TCB (Figure 5), the latter only yields an emission

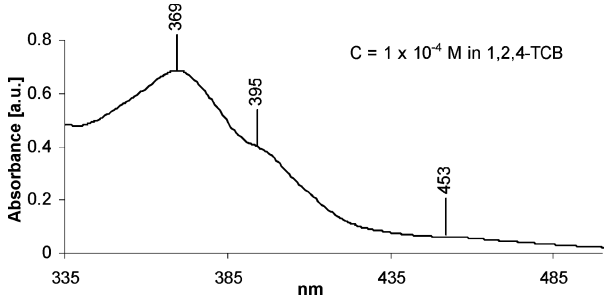

Figure 5. UV−Vis spectrum of HBC−$PhORf_{6,6}$ (**45**).

spectrum. Comparison with the emission spectrum obtained for HBC−$PhORf_{6,6}$ allowed estimation of the concentration of a saturated HBC−$PhORf_{4,8}$ solution to be ∼10 times lower than that of HBC−$PhORf_{6,6}$ (**45**).

The spectrum of this latter compound (Figure 6) deserves a comment: it originates from a concentration of 1×10^{-4} M and

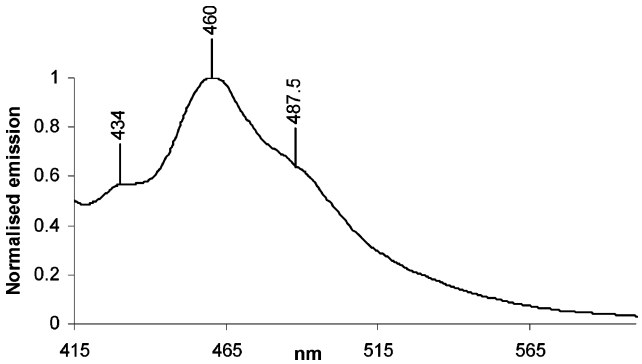

Figure 6. Emission spectrum of HBC−$PhORf_{4,8}$ (**44**) excited at 389 nm.

does not correspond to a saturated solution. Employing the extinction coefficient in the literature for unsubstituted HBC[3] (ϵ =

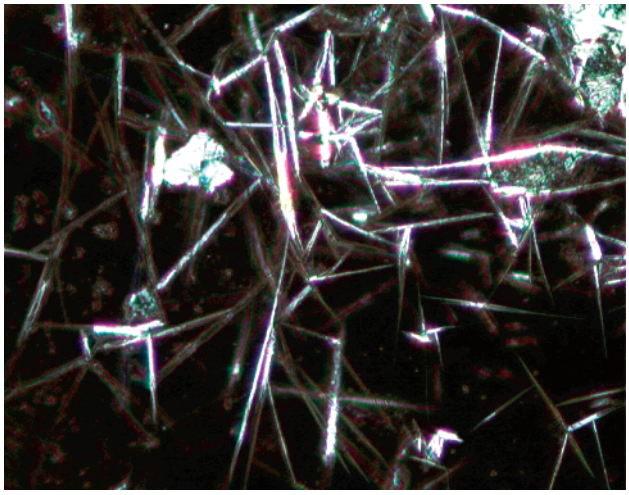

Figure 7. POM micrograph (×100) of the needlelike crystalline structures of **28** formed at 110 °C.

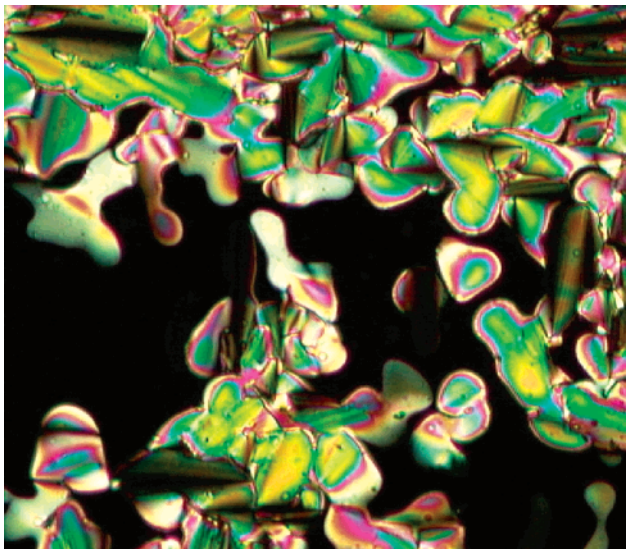

Figure 8. POM micrograph (×200) showing the columnar hexagonal texture of **28** formed at 217 °C.

114000), a concentration of 6×10^{-6} M would be calculated in our case. The obvious discrepancy can only be explained by the presence of higher molecular aggregates[34] which absorb at much longer wavelengths but which do not aggregate laterally and hence will not precipitate in our case due to the perfluorinated side chains.

Liquid Crystalline Properties

Polarization Optical Microscopy (POM) Investigation. The very high viscosity of the perfluorinated HBC products did not permit, when analyzed under POM, the growth of characteristic optical textures, allowing for an accurate mesophase identification except for HBC−$Rf_{4,8}$. Indeed, this compound revealed an interesting phenomenon: the yellowish amorphous powdered precipitate rapidly transforms to long needlelike crystalline structures on heating when reaching a temperature of ∼110 °C (Figure 7). These well-ordered arrangements disappear when reaching the transition to the mesophase (∼120 °C), which transformed and coalesced into a homogeneous texture reminiscent to that of a columnar hexagonal phase (Figure 8), and hardly reform when cooling the sample again. It is important to note that this particular organization of a product in the solid phase upon heating is reported for the first time for a HBC derivative and proves the high ability of these products to self-assemble in well-defined architectures. In contrast, the mesophase of HBC−$Rf_{6,6}$ is formed from a succession of various crystalline phases, and at a lower temperature than that of HBC−$Rf_{4,8}$.

Differential Scanning Calorimetry (DSC) Study. The thermal behavior of all these new HBCs was also studied by TGA and DSC with a heating and cooling rate of 20 °C/min. The products started to decompose in air at 300 °C before clearing in the isotropic liquid, the temperature of which could not be determined. All the HBCs that have been synthesized herein are mesomorphic, with transition temperatures strongly influenced by the structure of the mesogen, i.e., the size of the aromatic ring, and the nature and length of the side chains. For example, the insertion of a phenyl group between the HBC core and the perfluoroalkylated chains in HBC−$PhRf_{2,8}$ (**20**) increases the liquid phase transition temperature by ∼60 °C as compared to HBC−$Rf_{2,8}$ (**19**) (Table 2, entries 1 and 2). Concerning HBC−$Rf_{4,8}$ (**28**) and HBC−$Rf_{6,6}$ (**29**) (entries 3 and 4, respectively), both showed a mesophase at much lower temperature. Moreover, the phase transition temperature of the latter is lower by ∼10 °C as a reason for the presence of two additional methylene carbons that make the molecule more flexible. Entries 5 and 6 show that both HBC−$PhORf_{4,8}$ (**44**) and HBC−$PhORf_{6,6}$ (**45**) have comparably high transition temperatures with a melting into the mesophase above 220 °C, and this can be explained again by the extension of the flat core as well as the use of alkoxy chains. A minor decrease of the transition temperatures was also observed between these two extended HBC species as in the case of HBC−$Rf_{4,8}$ and HBC−$Rf_{6,6}$ (**28**, **29**).

However, it is important to note that the introduction of the perfluoroalkylated chains increases the rigidity of the molecule[29] which, hence, leads to different phase transition behavior from their peralkylated homologues.[38] The high ratio of CF_2/CH_2 in HBC−$Rf_{2,8}$ (**19**) results in an additional crystallization phase and increases the phase transition temperature (T_m) by ca. 56 °C with respect to the hexadecyl HBC derivative[39] (T_m = 124 °C). Likewise, reducing the CF_2/CH_2 ratio causes less rigidity and, consequently, a higher degree of freedom of the aliphatic part, which decreases the difference of the phase transition temperature between the hexadodecyl HBC[12] (T_m = 107 °C) with respect to HBC−$Rf_{4,8}$ (**28**, T_m = 120 °C) and approaches the same value to that of HBC−$Rf_{6,6}$ (**29**, T_m = 109 °C).

Structural Investigation of the Mesophases by Small-Angle X-ray Diffraction. Identification and unequivocal assignment of the mesophases was finally achieved by small-angle X-ray diffraction on powder samples for all the compounds. Qualitatively similar X-ray patterns were obtained for the two structurally related compounds, namely, HBC−$Rf_{6,6}$ (**29**) and HBC−$Rf_{4,8}$ (**28**), that both exhibit a single mesophase (from 109 and 120 °C, respectively). In

(38) Percec, V.; Bera, T. K. *Tetrahedron* **2002**, *58*, 4031−4040.
(39) Debije, M. G.; Piris, J.; De Haas, M. P.; Warman, J. M.; Tomovic, Z.; Simpson, C. D.; Watson, M. D.; Muellen, K. *J. Am. Chem. Soc.* **2004**, *126*, 4641−4645.

Table 2. Phase Transition Temperatures, Enthalpy Changes, and Structural Assignments for Different HBC Derivatives[a,b]

entry	compound	phase transition temperature (°C) heating/cooling	ΔH (kJ mol^{-1}) heating/cooling	phase width (°C)	assignment
1	HBC-$Rf_{2,8}$ (**19**)	122/114	1.4/1.2		Cr_1 - Cr_2
		138/128	37.2/36	16	Cr_2 - Cr_3
		180/173	7.7/6.5	42	Cr_3 - Col_r
		∼300			Col_r - dec.
2	HBC-PhR$f_{2,8}$ (**20**)	227/223	66.4/60.5		Cr_1 - Cr_2
		236/235	19.8/14.2	9	Cr_2 - SmA
		∼300			SmA - dec.
3	HBC-$Rf_{4,8}$ (**28**)	82/(c)	6/(c)		Cr_1 - Cr_2
		120/103	58/52.6	38	Cr_2 - Col_h
		∼300			Col_h - dec.
4	HBC-$Rf_{6,6}$ (**29**)	50/(c)	4.6/(c)		Cr_1 - Cr_2
		109/98 (d)	48/46	18	Cr_2 - Col_h
		∼300			Col_h - dec.
5	HBC-PhOR$f_{4,8}$ (**44**)	182/(c)	3/(c)		Cr_1 - Cr_2
		216/207	18.7/19	34	Cr_2 - Cr_3
		222/215	6.3/25.6	6	Cr_3 - SmA
		∼300			SmA - dec.
6	HBC-PhOR$f_{6,6}$ (**45**)	ca. 200/(c)	(c)/(c)		Cr - Col_h
		∼300			Col_h - dec.

[a] Isotropic liquid was not observed, decomposition occurs above ∼300 °C. [b] Rate of heating and cooling is 20 °C/min. [c] Not determined. [d] Two peaks were obtained upon heating. With Cr, crystalline; Col_h, hexagonal columnar phase; Col_r, rectangular columnar phase with a pseudohexagonal symmetry; and SmA, smectic A phase.

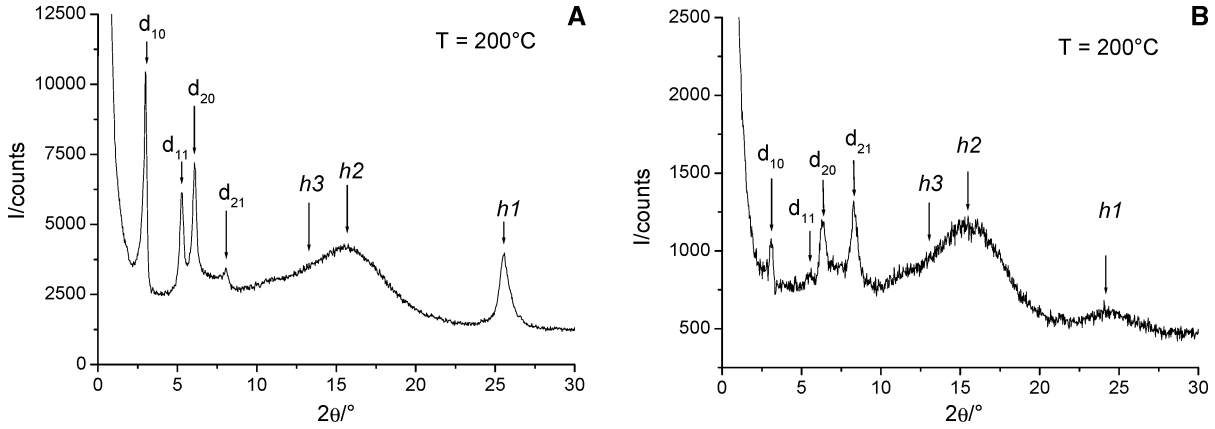

Figure 9. X-ray patterns of the Col_h phase at 200 °C for (A) HBC−$Rf_{6,6}$ (**29**) and (B) HBC−$Rf_{4,8}$ (**28**).

the small-angle region, four sharp Bragg reflections with the 1, $\sqrt{3}$, $\sqrt{4}$, $\sqrt{7}$ reciprocal spacing ratios were observed, typical for a 2D hexagonal lattice and corresponding to the indexation (hk) = (10), (11), (20), and (21) (Figures 9A and 9B). The presence of four reflections in the small-angle region of the X-ray pattern indicates that the hexagonal order is well-developed. In the angular range between $10° \leq 2\theta \leq 12°$, a few additional, less well-resolved reflections (forming a massif of peaks) could be seen, which correspond after indexation to the reflections (22) and (31). In the wide-angle region, some additional features were observed corresponding to various short-range interactions. First, at 3.5 Å, (*h1*), a fairly sharp peak for HBC−$Rf_{6,6}$ (**29**) and a slightly more diffuse scattering for HBC−$Rf_{4,8}$ (**28**) were observed, connected to the π stacking of the large flat aromatic HBC cores. This sharp signal for HBC−$Rf_{6,6}$ implies that the cores stack on top of each other along the columnar axis with a high regularity, whereas the broadening peak of HBC−$Rf_{4,8}$ (**28**) suggests that either the stacking is less regular, that it is not correlated over a long distance (vide infra), or that the PAH cores are slightly tilted with respect to the columnar axis. Thus, by simply changing the fluorinated fraction (from HBC−$Rf_{6,6}$ to HBC−$Rf_{4,8}$,), the order range of the stacking periodicity along the column may be controlled. Then, a broad and diffuse halo (*h2*) centered at around 5.6−5.9 Å, which reflects the liquidlike order of the perfluorinated chains, was visible for both samples. Finally, a very weak signal at 6.8−6.9 Å (*h3*), which corresponds to about twice the π-stacking distance ($h3 \approx 2h1$), may be due to some kind of dimerization (alternated stacking), though with a very short correlation length. Therefore, neither the nature of the mesophase nor the stability were drastically altered upon the variation of the fluorine volume fraction, and the lattice parameters were kept invariant over the entire mesomorphic temperature range up to the decomposition, the isotropization never being reached. The variation of the intercolumnar distance, defined as $a = 2/\sqrt{3}\langle d_{10}\rangle$ (Table 3), was indeed followed as a function of temperature for both compounds, and whatever the HBC considered, the hexagonal lattice does not shrink nor expand to a great extent from the melting up to 280 °C (variation is less than 1 Å -ESI). This observation implies that the packing mode remains fairly stable throughout the whole mesomorphic temperature range for both compounds. The only difference noted between these two compounds is that the lattice parameter of the hexagonal lattice decreases upon the increase of the fluorinated volume

Table 3. Thermal Behavior of the HBC and X-ray Characterization of the Mesophases[a,b]

entry	compound	d_{meas}/Å	I	indexation k	d_{calc}/Å	mesophase parameters measured at T	molecular volume at T (V_M)	N
1	HBC-$Rf_{2,8}$ (**19**)	27.2	M	20/11	27.2	T = 200 °C	V_M = 3300 Å^3	0.9
		15.7	M	31	15.7	Col_r-*p2gg*		
		12.3	M	41	12.5	a = 54.4 Å		
		10.3	W	42/51/13	10.3	b = 31.4 Å		
		5.8	br	*h*2		S = 854 Å^2		
						V_{cell} = 2990 Å^3		
2	HBC-$PhRf_{2,8}$ (**20**)	34.4	VS	001	34.45	T = 280 °C	V_M = 4010 Å^3	
		17.25	S	002	17.2	SmA		
		11.5	S	003	11.5	d = 34.45 Å		
		8.9	br	*h*		A_M = 120 Å^2		
		5.7	br	*h*2				
3	HBC-$Rf_{4,8}$ (**28**)	28.2	M	10	28.1	T = 200 °C	V_M = 3660 Å^3	0.9
		16.2	W	11	16.2	Col_h		
		14.0	M	20	14.05	a = 32.45 Å		
		10.6	M	21	10.6	S = 912 Å^2		
		6.9	br	*h*3		V_{cell} = 3190 Å^3		
		5.8	br	*h*2				
		3.5	br	*h*1				
4	HBC-$Rf_{6,6}$ (**29**)	29.15	S	10	29.0	T = 200 °C	V_M = 3460 Å^3	1.0
		16.65	S	11	16.75	Col_h		
		14.5	S	20	14.5	a = 33.5 Å		
		10.95	M	21	11.0	S = 971 Å^2		
		6.9	br	*h*3		V_{cell} = 3400 Å^3		
		5.8	br	*h*2				
		3.5	sh	*h*1				
5	HBC-$PhORf_{4,8}$ (**44**)	38.15	VS	001	37.9	T = 240 °C	V_M = 4310 Å^3	
		18.9	M	002	18.95	SmA		
		12.6	M	003	12.65	d = 37.9 Å		
		9.45	br	004	9.45	A_M = 114 Å^2		
		9.0	br	*h*				
		5.8		*h*2				
6	HBC-$PhORf_{6,6}$ (**45**)	33.8	S	10	33.7	T = 240 °C	V_M = 4110 Å^3	1.1
		19.45	VS	11	19.45	Col_h		
		16.8	VS	20	16.85	a = 38.9 Å		
		12.75	W	21	12.75	S = 1311 Å^2		
		5.5	br	*h*2		V_{cell} = 4590 Å^3		
		3.5	sh	*h*1				

[a] d_{meas} and d_{calc} are the measured and calculated diffraction spacings (d_{calc} is deduced from the following mathematical expression: $\langle d_{001}\rangle = (1/N_l)\sum_l d_{00l}.l$ where N_l is the number of 00*l* reflections for the SmA phase; $\langle d_{10}\rangle = (1/N_{hk})(\sum_{hk} d_{hk}.\sqrt{h^2+k^2+hk})$, where N_{hk} is the number of *hk* reflections for the Col_h phase). *I* is the intensity of the reflection (VS, very strong; S, strong; M, medium; br, broad; sh, sharp). 00*l* and *hk* are the indexations of the reflections corresponding to SmA and Col_h phases. *d* is the smectic periodicity ($d = \langle d_{001}\rangle$). A_M is the molecular area ($A_M = V_M/d$). *a* is the lattice parameter of the Col_h phase ($a = (2/\sqrt{3})\langle d_{10}\rangle$). *S* is the columnar cross-sectional area ($S = a\langle d_{10}\rangle$ for Col_h and 1/2*a.b* for Col_r). V_{cell}: volume of the hexagonal cell (*h1.S*), i.e., slice of column 3.5 Å thick. The molecular volume is defined by[44] $V_M = V_{HBC} + 6(nV_{CH_2} + mV_{CF_2})$ or $V_M = V_{HBC-Ph} + 6(nV_{CH_2} + mV_{CF_2})$, V_{HBC} = 650 Å^3, and V_{HBC-Ph} = 1220 Å^3. $V_{CH_2}(T) = 26.5616 + 0.02023T$ (T in °C, T_0 = 25 °C) and $V_{CF_2}(T) = 40.815 + 0.03318T$ (T in °C, T_0 = 22 °C). *N* is the number of molecules per V_{cell} ($N = (V_{cell}/V_{mol})$. [b] Col_h, hexagonal columnar phase; Col_r, rectangular columnar phase with a pseudohexagonal symmetry; SmA, smectic A phase.

fraction (*a* of HBC−$Rf_{6,6}$ is about 1−2 Å larger than *a* of HBC−$Rf_{4,8}$), in agreement with a slight tilt of the terminal rigid fluorinated segments with respect to the molecular HBC plane in the latter compound. An estimation of the molecular volumes permits verification that considering a stacking periodicity (i.e., a slice of column) of about 3.5 Å, deduced from the sharp scattering, about one single molecule can fit such a columnar stratum. Again, a small shift is observed for the compound with the highest volume fraction of fluorinated content, and when the temperature increases, suggesting that the molecules are slightly more apart from each other (the unit cell is more stretched), leading to a less efficient stacking. This may be due to the noncorrelated tilt of the molecular plane with respect to the columnar axis, resulting from a less efficient registry between each columnar stratum: the chains are more rigid and bulky and force the rigid cores to tilt to compensate this steric effect. Thus, to summarize, HBC−$Rf_{6,6}$ (**29**) compounds likely stack on top of each other, within an alternated manner in order to form flat dimeric assemblies in agreement with the sharp peak *h1* (compatible with the strong π interactions), and the weak peak *h3* (corresponding to the thickness of the dimeric species), whereas for HBC−$Rf_{4,8}$ (**28**), the columns are formed from the stacking of randomly tilted rigid cores due to relative bulkiness of the chains, as shown in the X-ray pattern by the flattening of both *h1* and *h3*, and the decrease of the lattice parameter. Note that another common feature for the X-ray patterns of both compounds was the increase of intensity of the fundamental reflection (10) as the temperature was raised. This is likely connected to the modification of the electronic density due to the presence of the fluorinated chains, when compared to the peralkylated analogues. This results in the modification of the electronic contrast between the different molecular parts, the electronic density of the zone occupied by fluorinated parts, and that of the PAH being similar.

Decreasing the chain length (**19**, HBC−$Rf_{2,8}$) led to an enhancement of the crystalline phases stability (observation

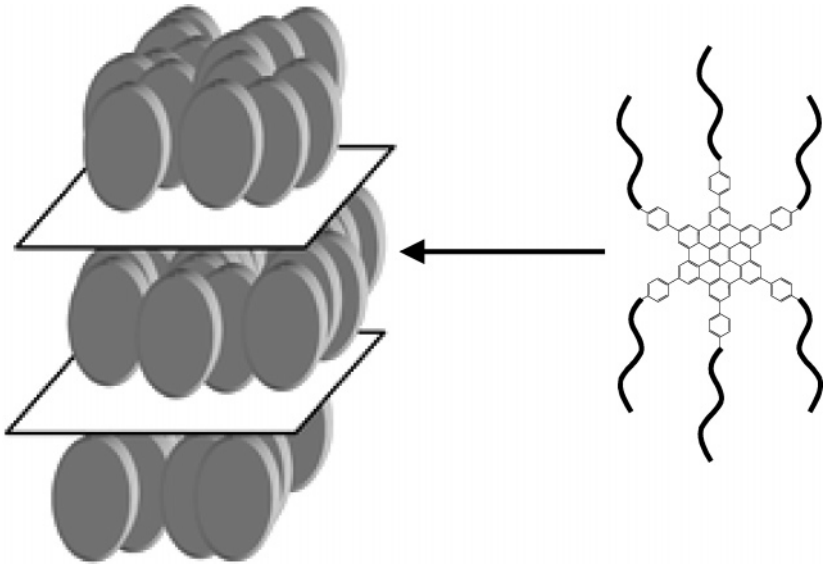

Figure 10. Mesomorphic structure (SmA) of HBC−PhRf$_{2,8}$ (**20**) and HBC−PhORf$_{4,8}$ (**44**).

of a rich crystalline polymorphism and high melting point at 180 °C) and to a subtle change of the mesophase symmetry. Here again, the isotropization could not be observed. X-ray diffraction only showed the diffuse scattering halo at 5.7−5.8 Å, associated with the liquidlike order of the perfluorinated chains, and a broad one at ca. 3.5 Å in the wide-angle area, along with some additional sharp reflections in the small-angle part. Similarly to **28** (HBC−Rf$_{4,8}$), this signal at 3.5 Å corresponding to the π stacking is very weak and can hardly be seen, in agreement with the hypothesis that an important fluorinated volume fraction forces the flat aromatic core to tilt with respect to the columnar axis. Four reflections were observed, for which the positions remain almost unchanged within the stability temperature domain (T = 200−280 °C), and were successfully indexed into a rectangular lattice with a pseudohexagonal symmetry (Col$_r$ phase, $a/b = \sqrt{3}$). The number of molecules per columnar slice 3.5 Å thick is about 0.9. This shows again that the cell is slightly too small to contain exactly one molecule and is probably due to the rigidity of the chain as for HBC−Rf$_{4,8}$ (**28**). In this case, to compensate the shrinkage of the 2D lattice, the molecule also tilts and thus the cell is stretched along the column.

For the compound HBC−PhRf$_{2,8}$ (**20**), only one mesophase can be detected at very high temperature. The phase is characterized by a series of three sharp small-angle reflections in the ratio 1:2:3 corresponding to a layered structure. Note that the low-temperature adjacent crystalline phase has also a lamellar structure, with a very similar periodicity. A diffuse halo is also observed at 5.7 Å, corresponding to the liquidlike state of the perfluorinated chains, and another weak one around 9−10 Å, maybe corresponding to some loose interactions between molecules. In this system, the integrity of the columns seems to be lost since neither lateral registry nor any stacking periodicity could be observed. The molecular area of ca. A = 120 Å^2 ($A = V_M/d$), corresponds to about three perfluorinated chains ($A = 3 \times 40$ Å^2, close to the cross section of one CF_2 group calculated to ca. 39 Å^2 at 280 °C) in their more stretched conformation, i.e., when the chains are aligned along the normal to the layers. If one estimates a lateral distance of ca. 24 Å, a sensible distance considering that by modelization, the diameter of the rigid core is close to ca. 22 Å, we can propose an arrangement of these molecules into a smectic A-type phase, with the rigid cores being slightly tilted in the layers, but without orientational tilt order. Thus, the discoid compounds are located into layers, with three side chains pointing up and the three other side chains pointing down. Due to the overall rectangular shape of the molecules, the rotation around the molecular axis parallel to the layer normal is strongly reduced, even hindered, likely leading to some local biaxiality of the smectic phase.[40] This structure is further stabilized by the strong microsegregation between the various incompatible parts, i.e., core structure and perfluorinated chains. Similarly, HBC−PhORf$_{4,8}$ (**44**) shows exactly the same thermal behavior and X-ray pattern, thus supporting the formation of a similar lamellar structure upon increasing the molecular size, and thus the same model as that described above holds for this compound too. Surprising, however, was the detection of a Col$_h$ phase for the compound with the different volume fraction of the fluorinated part in the chain. Indeed, at a temperature above 200 °C, the compound HBC−PhORf$_{6,6}$ (**45**) gave rise to a hexagonal columnar phase as proved by X-ray diffraction. This result was not expected considering the thermal behavior of the two related compounds just described. This may be linked to the greater flexibility of the longer methylene spacer as compared to that of HBC−PhORf$_{4,8}$ (**44**), which forces the fluorinated tails to adopt another conformation and, therefore, to the overall molecular disk to favor a columnar Col$_h$ phase formation rather than a lamellar arrangement (Figure 10).

It is worthwhile to note that the results shown herein are in good agreement with the ones reported for the hexadodecyl phenyl spaced HBC (HBC−PhC$_{12}$) that exhibits a much looser columnar packing than its non-phenyl spaced homologue (HBC−C$_{12}$).[34] Nonetheless, in the cases of HBC−PhRf$_{2,8}$ (**20**) and HBC−PhORf$_{4,8}$ (**44**), both compounds have

(40) Hegmann, T.; Kain, J.; Diele, S.; Pelzl, G.; Tschierske, C. *Angew. Chem., Int. Ed.* **2001**, *40*, 887−890.

the highest CF_2/CH_2 ratio and relatively superior molecular densities, which influence drastically their self-assembly, leading, thus, to a more significant change in their mesophases (SmA). As a result, the introduction of perfluoroalkylated groups into large discotic PAHs paves the way toward the possibility of tuning their liquid crystalline phases into various ones which have been detected, so far, for smaller aromatic molecules bearing fluorinated groups.[41−43]

Conclusion

We succeeded in synthesizing new HBC molecules in which the perfluoroalkylated chains were separated from the π-stacking core either by aliphatic spacers of different lengths and/or phenyl and phenoxy spacers. Lateral interaction between columnar aggregates was reduced as compared to HBCs with purely aliphatic chains but, to the contrary, the transition temperatures for comparable compounds were raised instead of lowered. We explain this fact by the existence of much longer columnar aggregates in our case, which compensate for the reduced lateral interactions. Evidence for this hypothesis comes from the observation of spontaneous formation of needlelike structures during heating and the predominate presence of highly aggregated perfluoroalkylated HBCs in homogeneous solutions. This can also be supported by the high stability of the columnar arrangements as revealed by the variable temperature XRD investigation we carried out for selected perfluorinated HBC species. Furthermore, we showed that self-organization of these disc-shaped molecules whose aliphatic analogues are known to form highly packed columnar stacks exclusively can be tuned to different mesomorphic phases by slightly altering the core size and changing the type of the side groups substituents, mainly, the ratio between the fluorinated and the aliphatic chains.

Acknowledgment. We thank the Swiss National Science Foundation National Research Program: Supramolecular Functional Materials (NRP 47-057425) for supporting this work.

Supporting Information Available: Experimental procedures and powder X-ray diffraction data (PDF). This material is available free of charge via the Internet at http://pubs.acs.org.

(41) Tschierske, C. *J. Mater. Chem.* **1998**, *8*, 1385−1508.
(42) Cheng, X.; Das, M. K.; Diele, S.; Tschierske, C. *Langmuir* **2002**, *18*, 6521−6529.
(43) Cheng, X.; Das, M. K.; Baumeister, U.; Diele, S.; Tschierske, C. *J. Am. Chem. Soc.* **2004**, *126*, 12930−12940.
(44) Goddard, R.; Haenel, M. W.; Herndon, W. C.; Krueger, C.; Zander, M. *J. Am. Chem. Soc.* **1995**, *117*, 30−41.